STEM CELLS AND DEVELOPMENT
Volume 19, Number 11, 2010

DOI: 10.1089/scd.2009.0498

Efficient Differentiation of Human Embryonic Stem Cells into Functional Cerebellar-Like Cells

Slaven Erceg,[1,*] Mohammad Ronaghi,[1] Ivan Zipancic,[2] Sergio Lainez,[3] Mireia Gárcia Roselló,[1] Chen Xiong,[1] Victoria Moreno-Manzano,[1] Fernando Javier Rodríguez-Jiménez,[1] Rosa Planells,[3] Manuel Alvarez-Dolado,[4] Shom Shanker Bhattacharya,[2] and Miodrag Stojkovic[1,†,‡]

The cerebellum has critical roles in motor and sensory learning and motor coordination. Many cerebellum-related disorders indicate cell therapy as a possible treatment of neural loss. Here we show that application of inductive signals involved in early patterning of the cerebellar region followed by application of different factors directs human embryonic stem cell differentiation into cerebellar-like cells such as granule neurons, Purkinje cells, interneuron, and glial cells. Neurons derived using our protocol showed a T-shaped polarity phenotype and express similar markers to the developed human cerebellum. Electrophysiological measurements confirmed functional electrical properties compatible with these cells. In vivo implantation of differentiated human embryonic stem cells transfected with MATH1-GFP construct into neonatal mice resulted in cell migration across the molecular and the Purkinje cell layers and settlement in the internal molecular layers. Our findings demonstrate that the universal mechanisms involved in the development of cerebellum can be efficiently recapitulated in vitro, which enables the design of new strategies for cell replacement therapy, to study early human development and pathogenesis of neurodegenerative diseases.

Introduction

The cerebellum has been implicated primarily in motor learning and higher cognitive coordination, although the circuitry involved in these activities is not yet understood [1]. There are numerous cerebellar disorders and many of them are related to progressive neurodegeneration due to the loss or malfunction of neurons in cerebellum [2]. Replacement therapy of cerebellar neurons with human embryonic stem cell (hESC)–derived cells has a great promise; however, this strategy depends on the ability to induce differentiation of hESC into functional cells with specific cell fates as well as their delivery to specific brain regions. Several efforts have been made to generate regional specific neurons such as spinal motorneurons [3–5] or midbrain dopaminergic neurons [6–9] using ESCs. Recent studies showed that developmentally relevant signaling factors can induce differentiation of murine ESCs into midbrain/hindbrain progenitor cells and subsequently into cerebellar neurons [10,11]. Little information is available regarding the mechanisms of neural patterning and specification in the human developing cerebellum. During embryogenesis, the cerebellum arises from dorsal rhombomere 1 (r1) [12] along the anterior/posterior axis of the developing neural tube. The cerebellar territory depends on the formation and function of the isthmus [13], a well-described signaling center at the junction between the mesencephalon and metencephalon. As development proceeds, the cerebellar anlage gives rise to several classes of neurons: granule cells (GCs), Purkinje cells, Golgi cells, stellate cells, and basket cells. In rodents, GC precursors (GCPs), the most abundant cells of cerebellum, arise from the external granular layer (EGL) proceeding from the rhombic lip, the germinal zone of the most dorsal neuroepithelium of r1 at the boundary of the mesencephalon and metencephalon [14,15], indicating that the specification of GCPs occurs at a relatively early stage of cerebellar development. Rostral rhombic lip progenitors will become GCPs, and in some cases, they give rise also to ventral neurons in the rostral hindbrain

[1]Cellular Reprogramming Laboratory, [2]Cell Regeneration Laboratory, [3]Sensorial Biology Laboratory, Centro de Investigación Príncipe Felipe (CIPF), Valencia, Spain.
[4]CABIMER (Centro Andaluz de Biología Molecular y Medicina Regenerativa), Avda. Americo Vespucio s/n, Parque Científico y Tecnológico Cartuja, Sevilla, Spain.
*Present address: CABIMER (Centro Andaluz de Biología Molecular y Medicina Regenerativa), Avda. Americo Vespucio s/n, Parque Científico y Tecnológico Cartuja, Sevilla, Spain.
†Present address: Spebo Medical, Leskovac, Serbia.
‡Present address: Department of Human Genetics, Medical School, University of Kragujevac, Kragujevac, Serbia.

region [16,17]. This region is defined by expression of the transcription factor Math1 [18,19]. The generation of GCPs, which migrate from the rhombic lip to populate the EGL, is induced by bone morphogenetic protein (BMP) signaling [20]. Additionally, different extracellular and nuclear factors such as Wnt and Fgf signaling [21,22] proteins produced by the mes/met boundary seem to be important in establishing further regional identity in the neural tube. Here, mimicking in vivo signaling pathways we were able to generate functional cells with cerebellar characteristics from hESCs, which express specific markers and engraft after cell transplantation.

Methods

Cell culture

Primary hESC colonies (H1 or H9 lines; WiCell) were mechanically dispersed into several small clumps, which were cultured on fresh commercially available human foreskin fibroblasts (American Type Culture Collection) inactivated by mitomycin C in hECS medium containing knockout-Dulbecco's modified Eagle's medium (DMEM; Invitrogen), 100 μM β-mercaptoethanol (Sigma), 1 mM L-glutamine (Invitrogen), 100 mM nonessential amino acids, 20% serum replacement (Invitrogen), 1% penicillin–streptomycin (Invitrogen), and 8 ng/mL basic fibroblast growth factor (bFGF; Invitrogen). hESC medium was changed every second day. hESCs were passaged by incubation in 1 mg/mL collagenase IV (animal-free; Invitrogen) for 5–8 min at 37°C or mechanically dissociated and then removed to freshly prepared human foreskin fibroblast layer. The same results were obtained using 2 different hESC lines.

Differentiation toward cerebellar neural cells

To initiate differentiation and to form embryoid bodies (EBs), undifferentiated hESC colonies (Stage I) were detached and transferred to low-attachment plates (Costar). The EBs were formed after 1 day and maintained in hESC medium for 4 days (Stage II). The medium was changed every day. After this period the EBs were transferred to neural induction medium consisting of DMEM/F12 with glutamax (Gibco), N2 supplement (Gibco), and heparin (2 μg/mL). Human FGF8 (100 ng/mL) and retinoic acid (RA, 10 μM) (Sigma) were added and the EBs were cultured for an additional 7 days (Stage III). To induce further differentiation toward cerebellar neurons, the EBs were transferred to plates previously coated with laminin (2 μg/mL) and fibronectin (5 μg/mL) (Sigma) and further cultured in basal medium eagle (BME) medium (Invitrogen) supplemented with insulin, transferrin, selenite (ITS) (Gibco), human FGF8 (100 ng/mL), human FGF4 (100 ng/mL), and human bFGF (20 ng/mL) (Invitrogen) for 4 days. Then, the cells were cultured for an additional 5 days in DMEM/F12 medium supplemented with human FGF8 (100 ng/mL), human wingless-related MMTV integration site 1 (WNT1) (50 ng/mL), and WNT3A (50 ng/mL) (Stage IV). To promote further differentiation, we cultured the cells in BME medium supplemented with N2, B27 (Invitrogen), human BMP4 (50 ng/mL), human BMP6 (20 ng/mL), human BMP7 (100 ng/mL), and human growth differentiation factor 7 (GDF7) (100 ng/mL) for additional 8 days (Stage V). To induce axon growth and proliferation (Stage VI), the cells were then disaggregated, replated, and cultured for another 8 days in BME medium supplemented with N2 and B27, to which the following factors were added: human BMP4 (50 ng/mL), human BMP6 (20 ng/mL), human BMP7 (100 ng/mL), human GDF7 (100 ng/mL), human Sonic hedgehog (100 ng/mL), human neurotrophin 3 (NT3) (100 ng/mL), jagged 1 (JAG1) (20 ng/mL), human brain derived neurotrophic factor (BDNF) (100 ng/mL). The human growth factors FGF8, BDNF, BMP7, and WNT1 were purchased from Peprotech, and factors BMP4, BMP6, SHH, Wnt3a, JAG1, NT3, and FGF4 from R&D Systems. Figure 1 summarizes the differentiation/experimental protocol. Eight independent experiments were performed for each described method.

RNA extraction and reverse transcription–polymerase chain reaction analysis

Total RNA was extracted using High Pure RNA Isolation Kit according to manufacturer's instructions (Roche Diagnostics). cDNA was synthesized using High Capacity cDNA Archive Kit (Applied Biosystems). Amplification was performed on the cDNA using Taq polymerase (Invitrogen). Polymerase chain reaction (PCR) conditions included a first step of 3 min at 94°C, a second step of 35 cycles of 15 s at 94°C, a 30 s annealing step at 56°C, 45 s at 72°C, and a final step of 8 min at 72°C. Glyceraldehyde-3-phosphate dehydrogenase was used as a control gene to evaluate and compare the quality and quantity of different cDNA transcripts. Primer sequences will be provided upon request. As a positive control for developing brain and cerebellum, we used human total RNA Master Panel II (Clontech), from which we used human fetal brain total RNA pooled from 21 male/female Caucasian fetuses obtained from autopsy materials (ages 26–40 weeks), human whole brain total RNA pooled from 2 male Caucasians (ages 47–55 years), and human cerebellum total RNA (Clontech) pooled from 10 male/female Caucasians (ages 22–68 years).

Immunocytochemistry

At different stages of differentiation, the cells were washed in phosphate-buffered saline (PBS) and fixed with 4% paraformaldehyde in PBS for 10 min. Fixed cells were washed twice with PBS before staining. After permeabilization in 2% Triton and blocking in 1% bovine serum albumin for 30 min, primary antibodies were applied in blocking buffer for 2 h at room temperature. The cells were washed 3 times in blocking buffer before secondary antibody application. Secondary antibodies of goat anti-mouse Alexa conjugated, goat anti-rabbit Alexa conjugated (Molecular Probes) were diluted at 1:500 in blocking buffer and applied to cells for 1 h at room temperature. After 2 washes in PBS, mounting medium containing 4′,6′-diamidino-2-phenylindole was applied for nuclear staining. Cells were observed under the fluorescence microscope 5 (Axiowert). For negative controls, primary antibodies were omitted and the same staining procedure was followed. Also, nonrelevant antibodies that have the same immunoglobulin isotope as specific antibodies were used and no positive reaction was found. The following primary antibodies and dilutions were used: rabbit anti-Nestin (1:250; Millipore), rabbit anti-ATH1 (1:200; Millipore),

mouse anti-beta III tubulin-Tuj1 (1:2000; Abcam), rabbit anti-Zic1 (1:200; Abcam), rabbit anti-Zic2 (1:200; Millipore), rabbit anti-Zic3 (1:200; Millipore), rabbit anti-Gbx2 (1:200; Millipore), rabbit anti-pax6 (1:100; Millipore), rabbit anti-NeuroD (1:200; Millipore), rabbit anti-ZIPRO1 (RU49) (1:250; Applied Biosystem), anti-pcp2 (1:100; Abgent), rabbit anti-Kir3.2 [G protein-gated K^+ current (GIRK)] (1:100; Sigma), mouse Calbindin28K (1:100; Sigma), rabbit anti-pax2 (1:100; Invitrogen), rabbit anti-En1 (1:100; Millipore), rabbit anti-otx2 (1:250; Millipore), rabbit anti-PDE1C (1:200; Abcam), rabbit anti-BLBP (1:100; Abcam), rabbit anti–γ-aminobutyric acid 6αR (anti-GABA6αR) (1:200; Chemicon, Millipore), mouse anti-GAD67 (1:200; Sigma), rabbit anti-LHX5 (1:200; Chemicon, Millipore), rabbit anti-Ki67 (1:200; Abcam), mouse anti-Meis1 (1:250; Upstate), rabbit anti-GFP (1:500; Abcam), mouse anti-human nuclei (1:100; Millipore), rabbit anti-doublecortin (1:100; Millipore). The cytochemistry experiments were done at least 5 times with each hESC line. For image analysis, 8 microscopic fields from each samples were taken randomly using×20 objective. Two independent investigators counted the number of immunoreactive cells for each staining. The percentage of immunopositive cells was calculated dividing the number of specific cells by total cell number (4′,6-diamidino-2-phenylindole–stained cell nuclei).

Generation of MATH1-GFP hESCs

The MATH1-GFP transgenic hESCs were generated by introducing the Math1-enhancer–Venus-Neo/pBluescript SK^+ plasmid [11] into hESCs using Fugene. The expression of Venus (GFP) is driven by human β-promotor and mouse Math1 enhancer (AF218258), which has 75% homology with the human sequence of Math1 enhancer (AF 218259). Briefly, the undifferentiated hESC colonies were maintained on Matrigel (Sigma) in human fibroblast-conditioned medium for 3 passages. The cell colonies were transfected with 10 μg of plasmid. After transfection, the cells carrying the plasmid were selected with 200 μg/mL of Gentamicin (Sigma). Strong Venus expression was detected upon differentiation (Fig. 5). Three independent MATH1-hESC lines were generated and differentiated and Math1 induction efficiency was similar in all 3 lines.

Electrophysiology

All reagents were from Sigma, unless otherwise stated. For current recordings, an EPC-10 amplifier was employed (HEKA GmbH). The holding potential (V_h) was −70 mV in all cases. The bath solution consisted of the following components (in mM): 140 NaCl, 4 KCl, 2 $CaCl_2$, 10 HEPES, 5 glucose, 20 mannitol (pH 7.4). The electrode solution contained the following components (in mM): 144 KCl, 2$MgCl_2$, 10 HEPES, 5 EGTA (pH 7.2). The pipette resistance was 1.5–2 MΩ. Series resistance was compensated for >70% and leak subtraction was performed. Data were low pass-filtered at 3.3 kHz and sampled at 10 kHz. Applied pulse protocols and analysis were carried out by Pulse software (HEKA). Action potentials were evoked by applying a variable pulse of current (40–60 pA) to neurons in current-clamp configuration. In the voltage clamp configuration, squared pulse depolarization voltage steps were applied to −10 mV or to +60 mV from V_h. Tetrodotoxin (TTX) (Tocris Laboratories) at 1 μM was used to block TTX-sensitive voltage-dependent Na^+ channels. Replacement of K^+ by Cs^+ in the internal solution or external application of 2 mM 4-aminopyridine blocked outward currents. Receptor agonists: glutamate (Glu) at 100 μM, Glu at 100 μM plus glycine at 50 μM (Glu Gly), GABA at 100 μM, or acetylcholine (Ach) at 100 μM were tested. The antagonists bicuculline (Tocris Laboratories), 6-cyano-7-nitroquinoxaline 6,2-amino-5-phosphonopentanoic acid (AP5), and α-tubocurarine were examined on neurotransmitter-mediated currents at the same concentration as the agonists. Data were averaged and represented as mean ± standard error of the mean.

In vivo transplantation

Highly concentrated cell suspension (∼10×10^5 in 1 μL) of differentiated and sorted MATH1-GFP+ cells was front-loaded into bevelled glass micropipettes (∼50 μm diameter) that were prefilled with mineral oil and L-15 medium. Micropipettes were connected to a microinjector mounted on a stereotactic apparatus specially adapted for neonatal mice. Three- to 4-day-old CD-1 mice (Charles River Laboratories) were anesthetized by exposure to ∼4°C until pedal reflex was abolished. Anesthesia was maintained by performing surgery on a cold aluminium plate. A total of 10×10^4 cells per mouse in a 100–200 nL volume were injected at the following coordinates from lambda: cerebellum [0.5 mm anterior (A), 0.5 mm lateral (L), 1.0 mm dorsal (D)]. As a control, we injected an equivalent volume of heat-shocked "dead" cells. Grafted pups were returned to their mothers and analyzed after 4 weeks. After this period of time, the pups were deeply anesthetized (Nembutal; Abbot Laboratories) and perfused with 4% paraformaldehyde. We processed the tissue and cut 14-μm cryostat sections, which were immunostained with anti-EGFP antibodies and observed under the confocal microscope. All experimental animals were treated in accordance with the institute's Bioethical Committee.

Results

Differentiation of hESCs

To induce in vitro differentiation, hESC colonies were detached from a feeder layer and cultured in suspension as EBs for 4 days in the hESC growth medium (Fig. 1) following an additional 7 days in the motor induction medium (MIM) medium supplemented with RA and FGF8. In the normal development, the latter induces formation of an ectopic isthmic organizer and isthmocerebellar development via coexpression of OTX2 and GBX2 [23], 2 markers strongly expressed in Stage III (Fig. 2J). Also, after this period, real-time (RT)-PCR analysis showed that common neural markers including *NCAM*, *PAX6*, *TuJ1*, *PAX2* (interneuron marker for midbrain and caudal central nervous system [CNS]), and *HOXA2* (the marker responsible for delineation of r1, which gives rise to the cerebellum) were expressed (Fig. 2J). The expression of the same markers was found in human developing brain (Fig. 2J). The factors FGF8 and RA induce the expression of common granular cell markers *ZIC1*, *ZIPRO* (*RU49*), and *WNT1* but not *ATH1*, suggesting that FGF8 and RA are sufficient to induce expression of genes that establish the cerebellar anlagen (Fig. 2J). Further positional restriction in the generation of GCP seems to depend on patterning

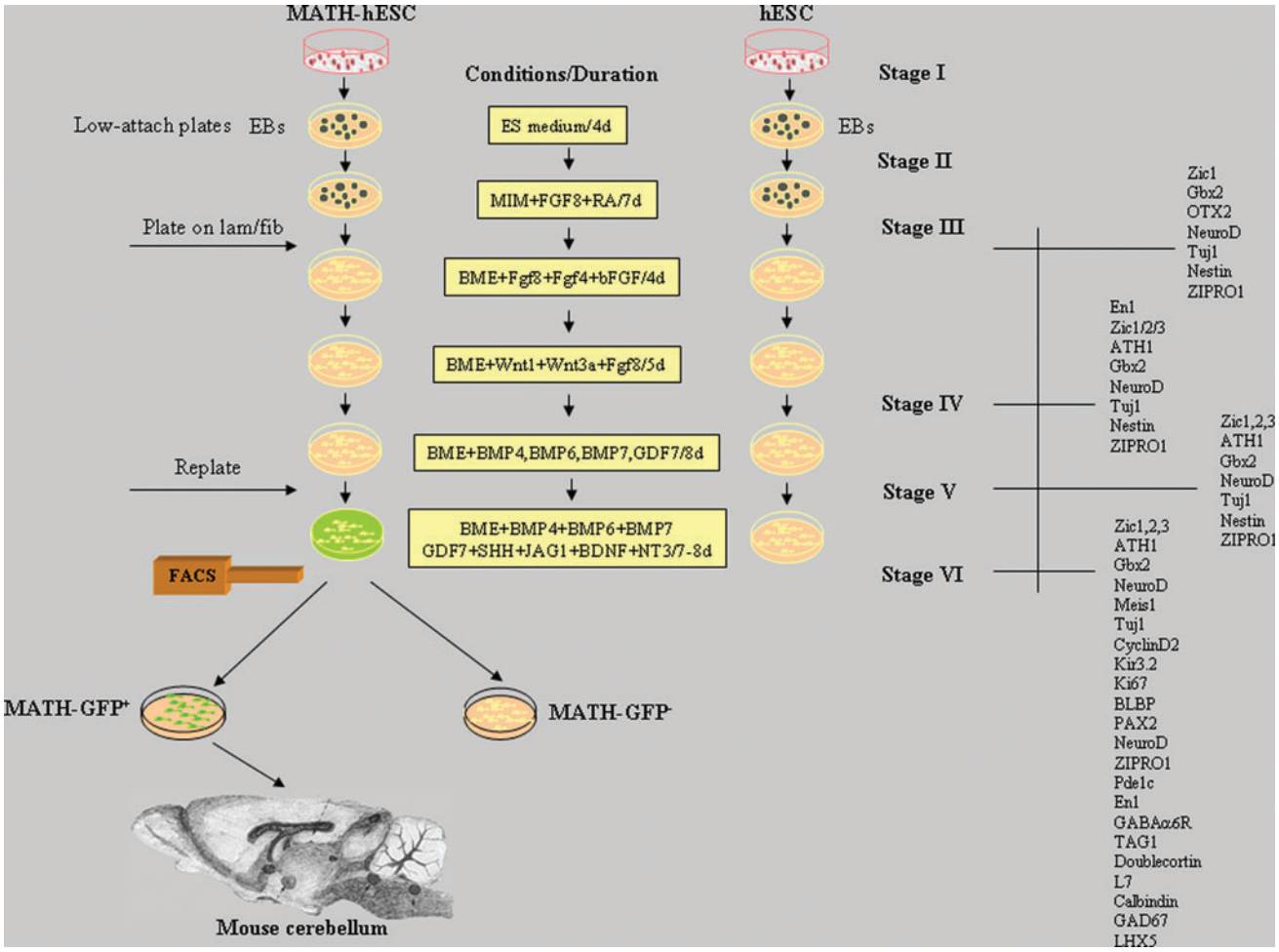

FIG. 1. Overview of the experimental schedule and the protocol of differentiation of hESCs toward cerebellar cells. hESCs or MATH1-hESCs were cultured in medium supplemented with soluble factors as described in the Methods section. The cellular marker genes expressed by differentiated hESCs detected by immunofluorescence and real time (RT)–polymerase chain reaction are indicated for each stage on the right side of the panel. After the Stage VI, cell sorting (FACS) was applied using differentiated MATH1-hESC line. The sorted cells were analyzed and transplanted to the developing mouse cerebellum. hESC, human embryonic stem cell; EBs, embryonic bodies. Color images available online at www.liebertonline.com/scd.

signals well known for their crucial role in establishment of the cerebellar primordium [24]. The expression of these transcription factor genes is under the control of inductive signaling involving different FGF and WNT proteins produced by cells at the mesencephalic/metencephalic boundary. To further characterize the patterns of gene expression and cell movement, we transferred the EBs in an adhesive culture system and chemically defined culture medium containing FGF8, FGF4, and bFGF for 4 days followed by addition of WNT1 and WNT3a for another 5 days (Stage IV). Treatment with FGFs, WNT1, and WNT3a induced the expression of common hindbrain marker *EN1* (Fig. 2A, J) as well as transcription factor *ATH1*, the rhombic lip GCP marker [25,26] (Fig. 2B, J). The function of this gene (together with ZIPRO [27]) is required for cerebellar GC generation and formation of the EGL [26]. Imunocytochemistry analysis after this differentiation stage confirmed the presence of the most important GCP markers. The cells were $ATH1^+$ ($46\% \pm 3\%$; Fig. 2B, I), $NESTIN^+$ ($84\% \pm 3\%$; Fig. 2C, I), $NEUROD^+$ ($62\% \pm 3\%$; Fig. 2D, I), $ZIC1^+$ ($75\% \pm 2\%$; Fig. 2E, H), $ZIC2^+$ ($72\% \pm 2\%$; Fig. 2F, I), $ZIC3^+$ ($74\% \pm 3\%$; Fig. 2G, I), and $GBX2^+$ ($65\% \pm 3\%$; Fig. 2H, I).

Several studies provide evidence that BMP-mediated inductive signals can promote further formation of granule neuron progenitors in vitro [10,20]. BMPs, with their dorsalizing effects [20,28], further continue the program of GC specification. We observed that treatment of cells only with BMP4 factor did not provide further differentiation of these cells as was the case with mouse ESCs [11] (data not shown). Addition of 4 members of the BMP family, BMP4, BMP6, BMP7, and GDF7, increases the expression of the main GPC markers. The expression of the most important cerebellar genes was maintained or increased and did not reveal the presence of other genes involved in further characterization of differentiated cerebellar cells (Fig. 2J). However, the expression of *GBX2* and *OTX2* was considerably decreased (Fig. 2J).

SHH signaling controls the development of cerebellum, induces the differentiation of Bergmann glia [29], and is required for the proliferation of GCPs. The GCP differentiation

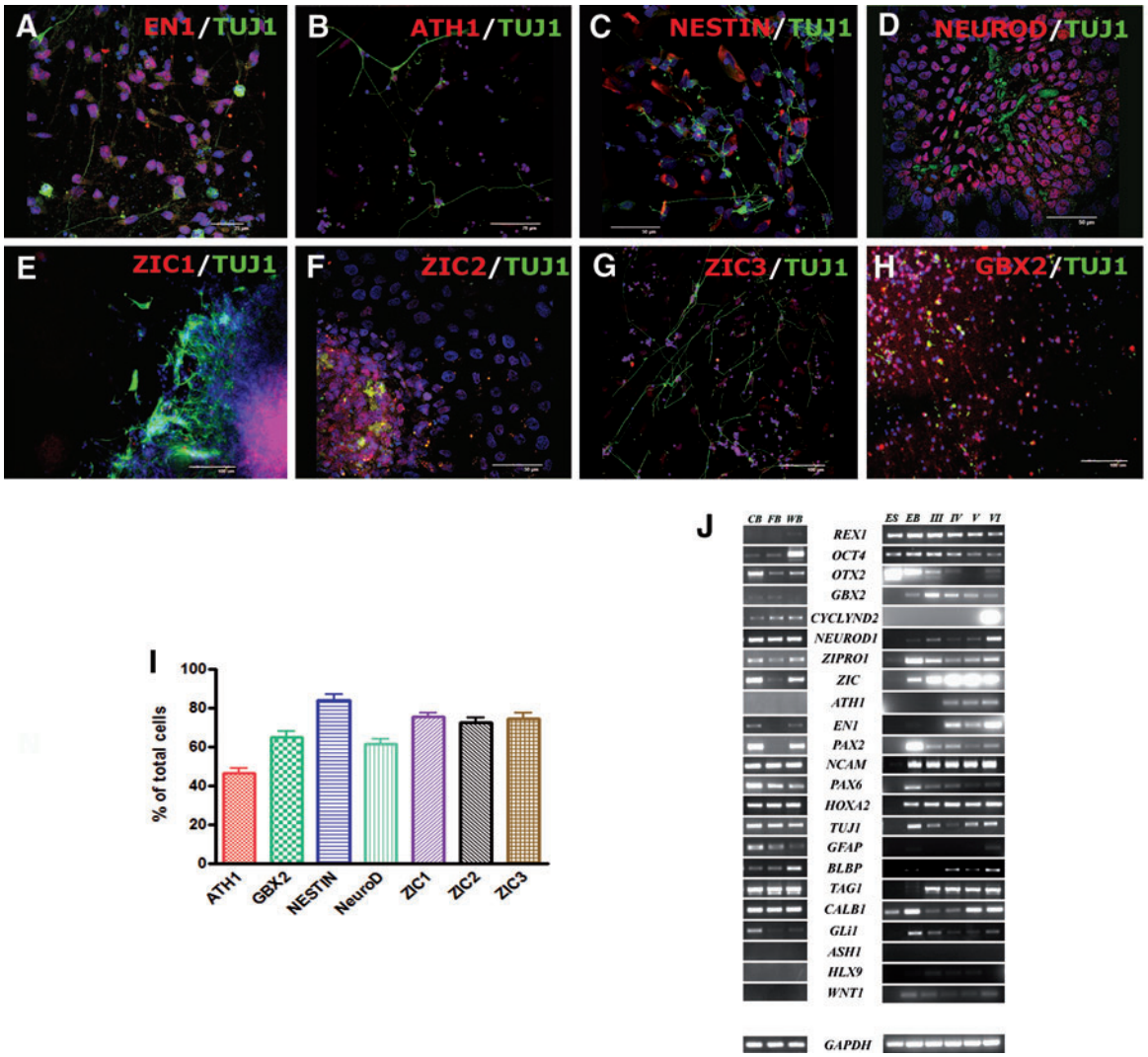

FIG. 2. Immunostaining of differentiated hESCs after treatment with FGF8, WNT1, and WNT3A (Stage IV). Differentiated hESCs express different cerebellar markers including EN1 **(A)**, ATH1 **(B)**, NESTIN **(C)**, NEUROD **(D)**, ZIC1 **(E)**, ZIC2 **(F)**, ZIC3 **(G)**, and GBX2 **(H)**. Blue indicates 4′,6-diamidino-2-phenylindole. The bars indicate the percentage of each marker according to total number of cells (4′,6-diamidino-2-phenylindole stained) **(I)**. The expression profile of all analyzed genes throughout the protocol is shown **(J)**. Data were averaged and represented as means ± SEM ($n = 5$). Scale bar: 50 μm. SEM, standard error of the mean; ES, human embryonic stem cells; EB, embryoid bodies; CB, human cerebellum; FB, fetal brain; WB, whole brain; GAPDH, glyceraldehyde-3-phosphate dehydrogenase. Color images available online at www.liebertonline.com/scd.

depends on ATH1, which acts by regulating the level of multiple components of the Notch signaling pathway [30]. To assess the mitogenic effects of SHH and Notch signaling in a further cerebellar phenotype, we cultured differentiating hESCs after Stage V in a medium supplemented with SHH and JAG1 in addition to the factors used in the previous step (Fig. 1). We included also BDNF and NT3, 2 neurotrophins involved in axonal growth of developing CG cells [31]. The outcome was a very rapid proliferation of differentiated cells, which is the most important characteristic of EGL cells in vivo after birth. The cell proliferation analysis revealed an important population of differentiated Ki67$^+$cells (22% ± 1%; Fig. 3K, R). The RT-PCR analysis showed that the applied factors induce expression of *CYCLIND2*, which is expressed in neonatal GCPs in the EGL (Fig. 2J). Continued expression of specific GCP markers including *ATH1*, *ZIC1-3*, *ZIPRO1*, and *PAX6* as well as *PAX2* was also observed (Fig. 2J). The cells also expressed *TAG1*, an axonal glycoprotein that positively regulates, besides tangential migration of cortical GABAergic interneurons, a subset of precerebellar neurons in the caudal hindbrain [32]. *GLI1* was expressed in Stage VI (Fig. 2J), confirming that the expression of the Shh target gene *GLI1* is restricted to proliferating GCP and Bergmann glia [33]. Finally, the majority of differentiated cells were ATH1$^+$ (39% ± 2%; Fig. 3A, B, R), MEIS1$^+$ (53% ± 2%; Fig. 3B, R), ZIPRO1$^+$ (74% ± 2%; Fig. 3C, R), ZIC1$^+$ (73% ± 2%; Fig. 3D, R), ZIC2$^+$ (76% ± 3%; Fig. 3E, R), ZIC3$^+$ (77% ± 2%; Fig. 3F, R), NEUROD$^+$ (76% ± 2%; Fig. 3G, R), PDE1C$^+$ (49% ± 2%; Fig. 3H, R), PAX6$^+$ (20% ± 2%; Fig. 3R), and GABAα_6R$^+$ (47% ± 1%; Fig. 3R). Cerebellar granule neurons normally express GIRK, which is involved in the neurotransmitter regulation of the excitatory input to the Purkinje

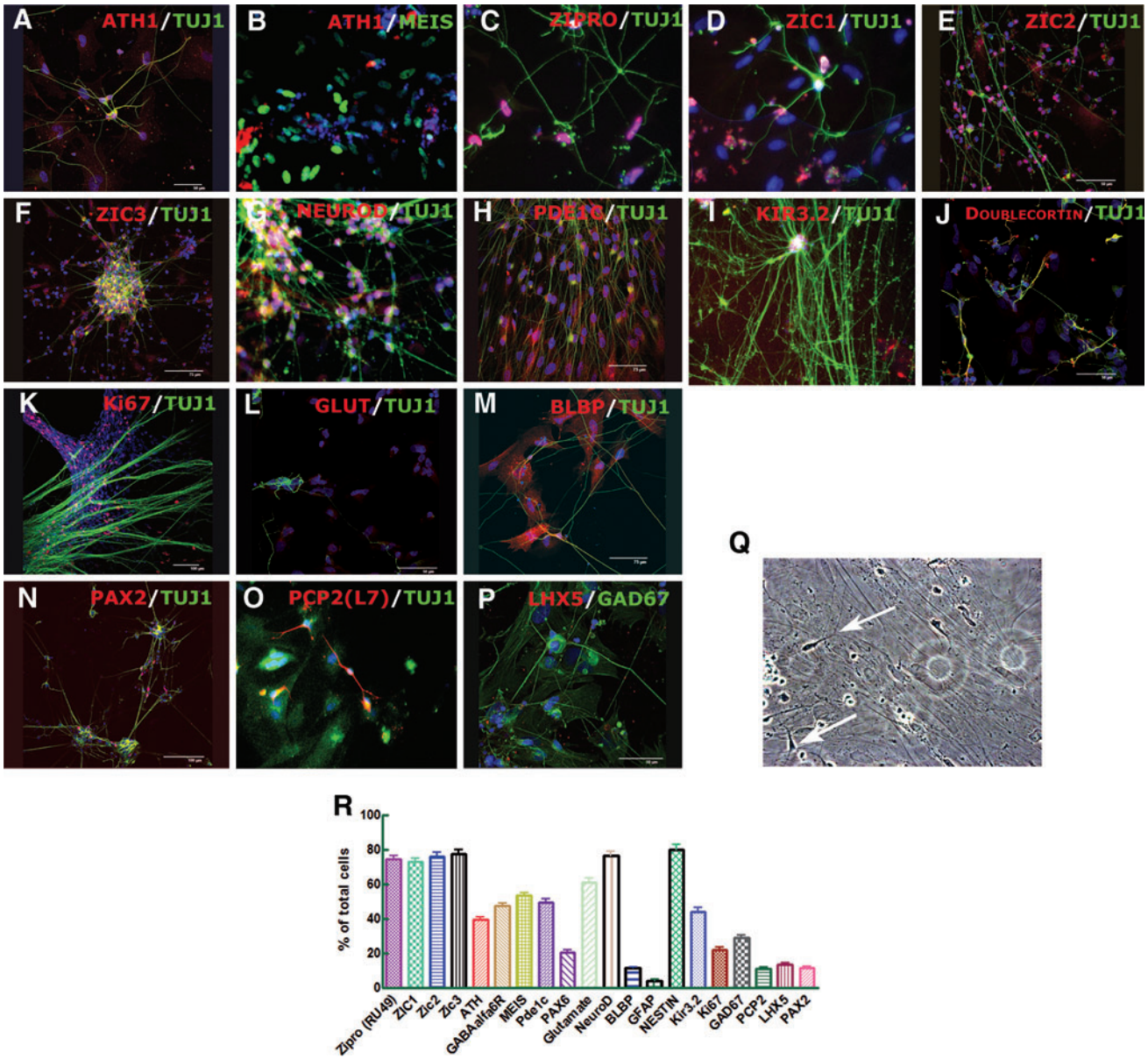

FIG. 3. The immunocytochemical analysis of differentiated cells after 7–8 days of culture with BMP4, BMP6, BMP7, GDF7, SHH, JAG1, BDNF, and NT3 (Stage VI). Differentiated hESCs coexpressed the granule neuron marker ATH1, with TUJ1 **(A)** and MEIS1 **(B)**. The cells also were positive to ZIPRO **(C)**, ZIC1 **(D)**, ZIC2 **(E)**, ZIC3 **(F)**, NEUROD **(G)**, PDE1C **(H)**, KIR3.2 **(I)**, DOUBLECORTIN **(J)**, Ki67 **(K)**, GLUTAMATE **(L)**, radial glia marker BLBP **(M)**, interneuron marker PAX2 **(N)**, and the Purkinje cell markers: PCP2 **(O)** GAD67 and LHX5 **(P)**. Differentiated hESCs also express neuronal marker class III β-tubulin (TUJ1; A, C–O). The generated neurons express typical "T-shaped" (indicated by arrows) phenotype **(Q)**. Number of cells for each marker analyzed by immunocytochemistry is shown **(R)**. Data were averaged and represented as means ± SEM ($n = 5$). Scale bar: 50 μm. Color images available online at www.liebertonline.com/scd.

fibers of the cerebellum [34], and DOUBLECORTIN, a marker for migrating GCs [35]. We observed that about 41% (44% ± 6%) of the cells were GIRK2$^+$ (KIR3.2, Fig. 3I, R) and DOUBLECORTIN$^+$ (Fig. 3J). An inhibitory neurotransmitter that can activate GIRK in CG neurons is GABA. About 36% (36% ± 4%) of cells were GABA$^+$ (not shown) and about 61% (61% ± 3%) of differentiated cells were glutamatergic (Fig. 3L, R).

A very exciting result was the formation of "T-shaped" axons characteristic for GC neurons [36] (Fig. 3Q), which suggests that cells, under our culture conditions, express genes and use signaling pathways required for the development of the polarity of wild-type CG neurons [37]. About 11% ± 1% of cells also expressed the Bergman cell marker *BLBP* (Figs. 2J and 3M) and interneuron marker *PAX2* (Figs. 3N, R). Immunocytochemical assays showed very weak expression of the astroglial marker GFAP (4% ± 1%; Figs. 2J and 3R) but also the presence of Purkinje cells expressing PCP2 (L7; 11% ± 1%; Fig. 3O, R), GAD67 (29% ± 1%; Fig. 3P, R), and LHX5 (13% ± 1%; Fig. 3P, R), which is a considerably higher yield compared with other protocols using murine ESCs [11]. High expression of *CALB1* (Fig. 2J) confirms the

efficiency of our protocol to generate Purkinje cells. To confirm the regional specificity of generated cells, RT-PCR analysis showed that the cells did not express other CNS markers such as *HB9* (spinal motoneurons), *ASH1*, *NG2* (oligodendrocytes, not shown), and *NKX2.2* (motoneurons) (Fig. 2J). We also observed continual decrease of main pluripotent markers (*OCT4* and *REX1*) throughout the protocol. The specificity of the protocol was additionally confirmed by the absence of cells of endodermal and mesodermal trophoblast lineage (not shown). Usage of other differentiation methods, such as medium conditioned by rat GCP, induced generation of cells that displayed expression phenotypes characteristic of mostly GCP cells and interneurons; however, the presence of high *OCT4* expression indicates that this treatment does not eliminate the undifferentiated cells (Supplementary Data and Supplementary Fig. S1, available online at www.liebertonline.com/scd).

Electrophysiology

Cells visually scored as neurons, with a mean capacitance of 9.5 ± 4.2 pF ($n = 89$), were recorded by the patch-clamp whole-cell method to characterize differentiated cultures. Neurons analyzed by electrophysiology represent the whole neuronal population in the mixture of generated cells. When held in current clamp configuration at $V_h = -70$ mV and a depolarizing current step of 40–60 pA for 150 ms was applied, virtually all cells ($n = 80$) showed 1 or more action potentials, and 30 of 80 cells showed 2 or more action potentials (Fig. 4A). The action potential spikes could be effectively and reversibly blocked by the application of the specific voltage-dependent Na^+-channel blocker TTX at 1 μM ($n = 6$). Voltage-dependent Na^+ currents were recorded in the voltage-clamp configuration upon a depolarizing voltage step of −10 mV ($n = 80$), which was readily blocked by TTX at 1 μM ($n = 13$). Voltage-dependent K^+ currents ($n = 80$) were measured at +60 mV, and $66\% \pm 7\%$ was blocked with 2 mM 4-aminopyridine ($n = 5$) (Fig. 4B).

We classified neuronal populations using neurotransmitter sensitivity to GABA, Glu, acetylcholine (Ach), and Glu plus glycine (Glu + Gly) (Fig. 4C–E). All the recorded neurons showed a marked response to GABA ($n = 44$), with a current density of 270 ± 155 pA/pF. In contrast, 34% of cells (10/29 cells) showed sensitivity to Glu + Gly, with a current density of 7.8 ± 6.4 pA/pF. Both N-methyl-D-aspartic acid (NMDA) and non-NMDA receptors contributed to the glutamatergic-induced currents because the NMDA receptor antagonist AP5 reduced the inward current generated by extracellular perfusion with Glu + Gly by ~50% (from 8.4 ± 5.4 to 4.2 ± 4.2 pA/pF, $n = 9$), whereas combined application of AP5 with the non-N-methyl-D-aspartic acid (NMDA) receptor antagonist 6-cyano-7-nitroquinoxaline 6 blocked ~71% of the current (from 10.9 ± 9.9 to 3.2 ± 2.2 pA/pF, $n = 8$). Interestingly, 48% (14/29 cells) contained nicotinic Ach receptors, which were readily blocked by the specific antagonist α-tubocurarine ($n = 4$).

MATH1-GFP construct

To monitor expression of a GCP-specific gene at each of the differential stages, we generated hESCs transfected with

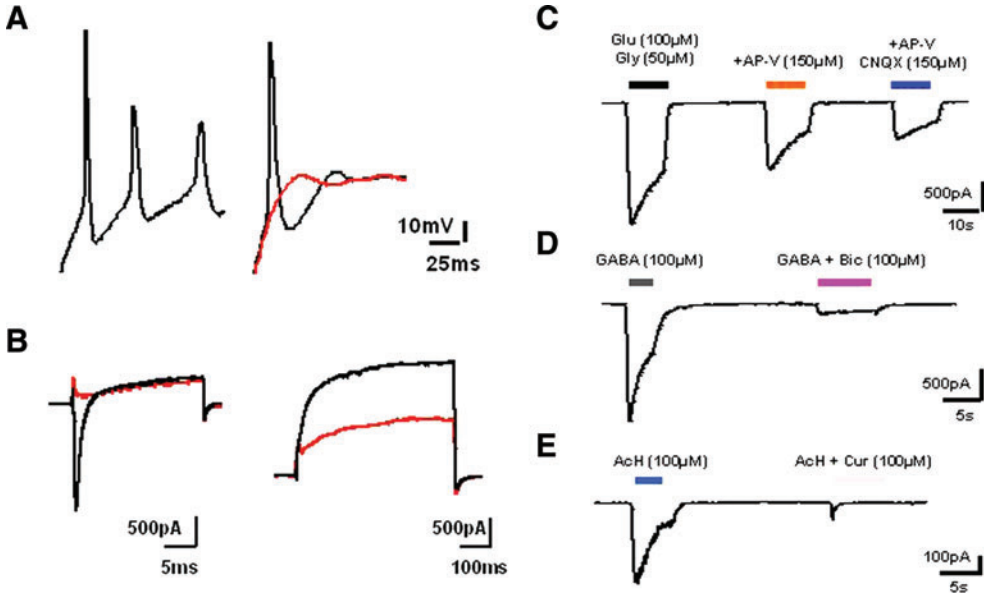

FIG. 4. **(A)** Excitability of the culture. Action potentials evoked by injection of small amounts of currents (40–60 pA). All the cells evoked 1 or more spikes ($n = 80$). Action potentials could be blocked by 1 μM tetrodotoxin (red trace). **(B)** Voltage-dependent currents. *Left:* Fast transient inward current evoked by a depolarizing step of −10 mV was fully blocked by 1 μM tetrodotoxin, a specific voltage-dependent Na^+ channel. *Right:* Outward current evoked upon a depolarizing step of +60 mV, which was partially blocked by 2 mM 4-aminopyridine. **(C–E)** Neurotransmitter sensitivity. (C) N-methyl-D-aspartic acid (NMDA) and non-NMDA glutamatergic currents obtained upon simultaneous perfusion with 100 μM Glu + 50 μM Gly (Glu + Gly) and blocked with 150 μM 2-amino-5-phosphonopentanoic acid (a.k.a. APV) or 2-amino-5-phosphonopentanoic acid + CNQX (both 150 μM). (D) $GABA_A$ receptor currents could be evoked with extracellular infusion of 100 μM GABA and specifically blocked by Bic. (E) Inward currents were evoked by infusion with 100 μM Ach and totally blocked with tubocurarine. Glu, glutamate; Gly, glycine; CNQX, 6-cyano-7-nitroquinoxaline 6; GABA, γ-aminobutyric acid; Bic, bicuculline; Ach, acetylcholine. Color images available online at www.liebertonline.com/scd.

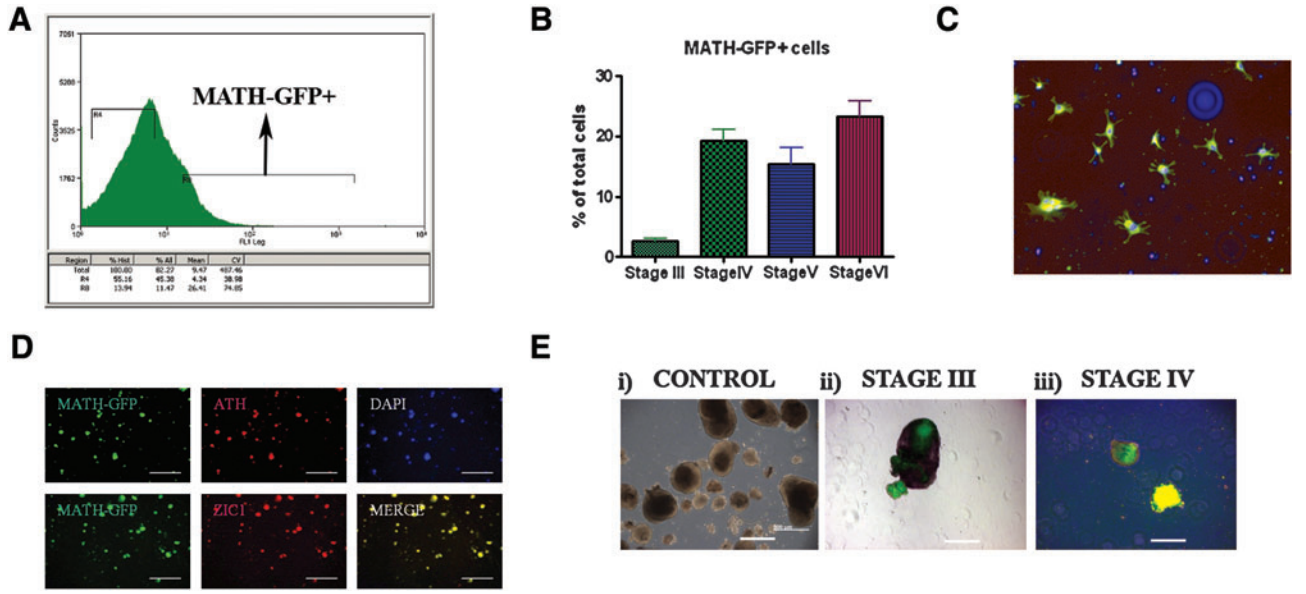

FIG. 5. Sorting and analysis of MATH1-GFP$^+$ cells. Typical sorting profile of 2 different fractions (GFP+ and GFP−) **(Aa)**. Negative control sorting: The EBs and cerebellar-like cells were maintained through all protocol but without differentiation factors **(Ab)**. The number of MATH1-GFP+ cells throughout the protocol (Stages III–VI) **(B)**. The MATH1-GFP+ cells sorted from Stage VI express the granule cell marker ATH1 and ZIC1 **(C, D)**. **(E)** EBs formed from MATH-hESCs: (**i**) MATH-hESCs grown without differentiation factors. EBs of MATH-GFP cells in (**ii**) Stage III and (**iii**) Stage IV (continued as EBs). RT–polymerase chain reaction analysis of sorted MATH1-GFP+ cells **(F)**. Data were averaged and represented as means ± SEM ($n = 5$). Scale bar: 50 μm. Color images available online at www.liebertonline.com/scd.

a GFP reporter gene expressed under control of the MATH1 enhancer. We sorted MATH1-GFP$^+$ cells by fluorescence-activated cell sorting in each differentiation step (Fig. 5A). Approximately 3% (3% ± 1%) of cells after adding FGF8 and RA were GFP$^+$, but about 19% (19% ± 3%), 15% (15% ± 5%), and 23% (23% ± 5%) (Fig. 5B, C, E) were in Stages IV–VI, respectively. Untreated MATH-hESCs showed GFP expression (Fig. 5A, E), but the cells were not positive for any of the GC markers (ATH, ZIC1, ZIC2).

The RT-PCR analysis of the cells generated at the end of our protocol showed that sorted MATH1-GFP$^+$ cells express several crucial GCP markers including *ATH*, *ZIC1*, *ZIPRO1*, *TUJ1*, *TAG1*, and *CYCLIND2*, but not *PAX2*, which is characteristic for interneurons (Fig. 5F). The lack of expression of specific sequence for VENUS-GFP construct in MATH1-GFP$^-$ cells provides the evidence that sorting was successful. After culturing of the sorted cells on laminin/fibronectin for 2 days, immunocytochemistry analysis confirmed some of the results obtained with RT-PCR. The majority of the cells (>99%) were ATH$^+$ and ZIC$^+$ (Fig. 5D). Granule neurons in vitro do not survive without supporting cells; therefore, these cells were used for cell transplantation.

Cell transplantation

To explore whether hESC-derived MATH1-GFP$^+$ cells can survive and integrate in the postnatal CNS, we implanted sorted and previously treated MATH-hESCs with the entire protocol (Stage VI). The cells were implanted in the mouse neonatal cerebellum of 7-day-old CD-1 pups at the level of EGL. The majority of surviving cells (14%–18% of total injected cells survived) did not reveal typical morphology for mature GCs (Fig. 6), consistent with the previous studies of cerebellar transplantation [10,11,20]. GFP staining revealed that cells migrated across the molecular layer, past the Purkinje cell layer, and settled in the internal granular layer, which is supposed to be the final destination of mature GCs. The presence of teratoma or other signs of

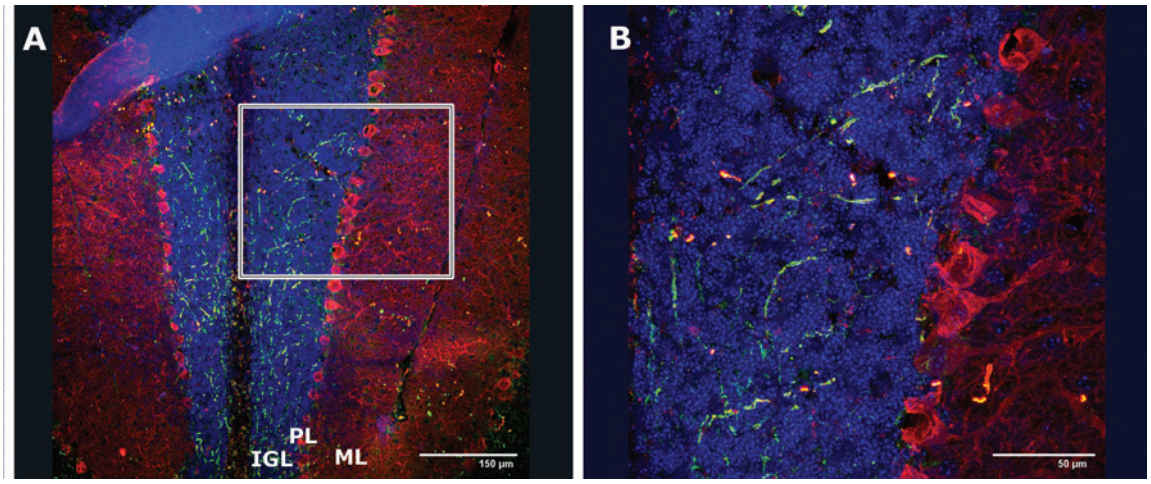

FIG. 6. Incorporation of differentiated hESCs into neonatal cerebellum. To test whether differentiated hESCs incorporate into cerebellar cortex, exit the cell cycle, and migrate into the IGL, either differentiated hESCs or granule cell progenitors from Stage VI differentiated from MATH1-GFP$^+$ hESCs and sorted were implanted in mouse pups. Two weeks after implantation, differentiated hESCs migrated and were detected by immunohistochemistry in the deeper layers of the developing cerebellar cortex. Postmigratory hESC-derived cells (GFP$^+$ cells) are seen in the IGL and PL (Purkinje cells were immunostained with Calbindin-red), where terminal differentiation occurs. **(B)** Electronic zoom 1×the area from the frame marked in **A**. IGL, internal granular layer; PL, Purkinje layer. Color images available online at www.liebertonline.com/scd.

tumorigenicity in any of the animals grafted were not observed.

Discussion

Our results show that application of inductive signals involved in the early patterning in the cerebellar region of the neural tube (FGF and WNT signaling and RA) followed by the factors involved in early GCP development (BMP4/6/7 and GDF7), mitogens (SHH and JAG1) and neurotrophins (BDNF and NT3), directs hESC differentiation into functional cerebellar cells (Figs. 1–3). The generated progenitors showed a GC phenotype expressing both markers of dorsal neurons (*MATH1* and *ZIC1*) and markers specific for GCs (*ZIPRO1*, *EN1*, *ZIC1-3*, *MEIS1*, *PDE1c*, *PAX6*, *TAG1*, *CYCLID2*, and *GABA*α_6*R*). In addition, cerebellar-like neurons expressed the T-shaped polarity phenotype of granule neurons (Fig. 3). We also observed the expression of the most important markers for Purkinje cells (Fig. 3): PCP2 (L7), LHX 5, GAD67, and CALBINDIN.

The molecular mechanisms underlying human development are complex and largely undefined. However, undifferentiated and differentiated hESCs offer an excellent in vitro tool to recapitulate mechanisms activated during early development. Previous developmental studies provided evidence that the formation of the cerebellar primordium depends on inductive signaling at the mes/met boundary [10,14,20,24]. Rhombic lip GCPs express the transcription factors MATH1 [25,26] and ZIPRO1(RU49) [27], and MATH1 function is required for GC generation and EGL formation [26,27]. Early cerebellar development also depends critically on inductive signaling involving canonical Wnt signaling [21] and FGF proteins secreted by cells of the isthmic region at this midbrain–hindbrain junction. Indeed, the inductive signals of FGFs, RA, and WNT used sequentially in our study were crucial for expression of human ATH1 in cerebellar EGL progenitors. These factors are well known for their crucial role in early neural development, where also RA and FGF8 signals induce differentiation of cells along the rostral/caudal axis [38,39]. Also, all these factors were required to induce the expression of *EN1* in differentiated hESCs, a gene required for the formation of the mes/met domain of the neural tube. Further differentiation of GCP progenitors and the generation of other cerebellar cell types, such as deep nuclei and Purkinje cells, depends on BMP-mediated dorsalizing signals [10,11,20]. GCPs expressing MATH1 arise close to the metencephalic roof plate, a source of BMP6, BMP7, and GDF7. Also, the dorsalizing activity of BMP4 on developing CNS tissue or differentiation of murine ESC toward GCP has been reported [20,28]. Our results show that treatment of differentiated hESCs with BMP4, BMP6, BMP7, and GDF7 is sufficient for the maintenance and increased expression of all cerebellar markers previously activated, but it is not crucial for further regional specification of cerebellar cells. By assessing the expression of Ki67 we found that differentiated cells showed high proliferation probably induced by SHH, JAG1, and Notch signaling, which plays instructive roles in the proliferation of granule neuron precursors and promotes the identities of several types of glial cells, including Bergmann glia [40].

Highly mitogenic factors BDNF and neurotrophins stimulate migration of individual GCs in vitro. In contrast, NT3 alters the morphology of outgrowth. High axonal growth observed in hESC-derived cerebellar cells confirms that regulation of neurotrophin receptors during cerebellar development is important for the timing and morphology of axonal growth [31,41].

With respect to efficiency, the induction of Purkinje cells, namely the yield of PCP2 (L7)$^+$ neurons, was higher when compared with another protocol using murine ESCs [11]. Very high expression of GAD67 as well as GABA itself indicates an early acquisition of this transmitter expression by cerebellar neurons, far in advance of their final positioning and establishment of synapses, confirming previous in vivo

findings [42]. In our study, cells positive for Purkinje markers did not coexpress CALBINDIN, which corroborates with a previous in vivo work [43] in which Purkinje cells began to exit the cell cycle before expressing the classical postmitotic Purkinje marker CALBINDIN.

The results in the present study are consistent with the studies done in mouse ESCs reported by Su et al [11] and Salero and Hatten [10], who introduced factors involved in the mechanisms of cerebellar development under in vitro conditions. Our results confirm that the same in vitro neural differentiation mechanisms can be applied using hESCs, but RT-PCR analysis revealed different timing of expression of some cerebellar markers during the differentiation of hESCs compared with murine counterparts. With this study we extend their previous findings showing expression of 2 additional GCP markers ZIC3 and GIRK3 and analyzing the functional electrophysiological activity of generated cells. We showed that differentiated neurons generated overshooting action potentials in response to depolarizing current injection. Further characterization of voltage-gated channels revealed the presence of Na^+ and K^+ channels as physiological markers of differentiation. Moreover, all recorded neuron-like cells responded to GABA, whereas only one-third responded to glutamate. When stimulated with GABA or Glu, newborn rat cerebellar explants of granule and Purkinje neurons elicit currents. In newborn mouse cerebellar slices, whole-cell recordings from Purkinje cell somata showed α-amino-3-hydroxy-5-methyl-4-isoxazolepropionic acid (AMPA) receptor–mediated spontaneous excitatory postsynaptic currents and $GABA_A$ receptor–mediated spontaneous inhibitory postsynaptic currents [44]. Similarly, in GCs, a part of the NMDA and non-NMDA excitatory components [44] showed $GABA_A$ receptors to mediate tonic inhibition [45]. Interestingly, nicotinic Ach receptors in ~50% neurons correlate with reports that link cerebellar nicotinic receptors with GABA and Glu neurotransmitter release [46] and therefore to influence neuronal activity like in autism [47].

Finally, we show that the previously designed MATH1 enhancer–directed GFP vector [11] could be a very useful tool to sort and purify the $MATH1^+$ cells (Fig. 5). As a result, we have isolated MATH1-GFP^+ cells (>99% of sorted GFP cells were ATH^+) as GCPs. This approach allowed us to isolate hESC-derived cerebellar progenitors, removing the population of undifferentiated hESC, as reflected in the absence of expression of the pluripotent markers *OCT4* and *REX1* in the cells from the sorted pool. This fact is one of the most important features of this system for its putative clinical application. Although this approach allowed us to reliably prepare and purify ATH^+ neurons from undifferentiated and other hESC-derived cells, the efficiency of this procedure may yet be significantly improved. Designing the genetic system that includes human ATH enhancer could be an approach for the future medical application of generated neurons. Nevertheless, these results suggest the utility of enhancer-based fluorescence for the isolation of specific phenotypes from differentiated hESC populations as a mean of purifying clinically appropriate cells.

We also successfully grafted MATH1-GFP^+ hESC-derived cerebellar cells in the postnatal mouse cerebellum, which resulted in cell survival and migration toward the region where the granular cells exert their function despite the cross-species nature of the grafts (Fig. 6), demonstrating the vitality of the cells and the robustness of our protocol, but further in vivo functionality analysis has to be performed.

Our study extends our knowledge about early human development and shows that it is possible to recapitulate human cerebellar development by using hESCs and human differentiation factors. For the first time, demonstration of the functional activity of differentiated hESC by patch-clamp analysis confirmed the cerebellar phenotype of generated neurons, which is a prerequisite for future applications in preclinical models of cerebellum-related diseases. Most importantly, improvement of this protocol for derivation of Purkinje cells is an important challenge for cell therapy for spinocerebellar atrophy diseases [48]. Although the road to the clinical application of hESC-derived cerebellar precursors remains extremely challenging, the ability to generate unlimited numbers of pure granular or Purkinje cell progeny and the capacity for in vivo survival and integration in the developing and adult cerebellum are important first stages in this journey.

Acknowledgments

The authors are thankful to Dr. Majlinda Lako, Dr. Lyle Armstrong, and Richard Griffeth for critical reading; Laura Nuñez Arrufat, Maria Amparo Pérez-Aragó, and Maria Gomez Lopez for their excellent technical support. This work was supported by funds for research in the field of regenerative medicine from the Regional Government Health Department (Generalitat Valenciana) and the Instituto Carlos III belonging to the Spanish Ministry of Health and Consumer Affairs, and through grants from the Spanish Ministry of Science and Innovation (SAF2007-63193) and La Marató (TV3 070330).

Author Disclosure Statement

No competing financial interests exist.

References

1. Middleton FA and PL Strick. (1998). The cerebellum: an overview. Trends Neurosci 21:367–369.
2. Rossi A, V Caracciolo, G Russo, K Reiss and A Giordano. (2008). Medulloblastoma: from molecular pathology to therapy. Clin Cancer Res 14:971–976.
3. Erceg S, S Lainez, M Ronaghi, P Stojkovic, MA Perez-Arago, V Moreno-Manzano, R Moreno-Palanques, R Planells-Cases and M Stojkovic. (2008). Differentiation of human embryonic stem cells to regional specific neural precursors in chemically defined medium conditions. PLoS ONE 3:e2122.
4. Lee H, GA Shamy, Y Elkabetz, CM Schofield, NL Harrsion, G Panagiotakos, ND Socci, V Tabar and L Studer. (2007). Directed differentiation and transplantation of human embryonic stem cell-derived motoneurons. Stem Cells 25:1931–1939.
5. Li XJ, ZW Du, ED Zarnowska, M Pankratz, LO Hansen, RA Pearce and SC Zhang. (2005). Specification of motoneurons from human embryonic stem cells. Nat Biotechnol 23:215–221.
6. Cho MS, YE Lee, JY Kim, S Chung, YH Cho, DS Kim, SM Kang, H Lee, MH Kim, JH Kim, JW Leem, SK Oh, YM Choi, DY Hwang, JW Chang and DW Kim. (2008). Highly efficient and large-scale generation of functional dopamine neurons from human embryonic stem cells. Proc Natl Acad Sci USA 105:3392–3397.

7. Iacovitti L, AE Donaldson, CE Marshall, S Suon and M Yang. (2007). A protocol for the differentiation of human embryonic stem cells into dopaminergic neurons using only chemically defined human additives: studies in vitro and in vivo. Brain Res 1127:19–25.
8. Ko JY, CH Park, HC Koh, YH Cho, JH Kyhm, YS Kim, I Lee, YS Lee and SH Lee. (2007). Human embryonic stem cell-derived neural precursors as a continuous, stable, and on-demand source for human dopamine neurons. J Neurochem 103:1417–1429.
9. Yang D, ZJ Zhang, M Oldenburg, M Ayala and SC Zhang. (2008). Human embryonic stem cell-derived dopaminergic neurons reverse functional deficit in parkinsonian rats. Stem Cells 26:55–63.
10. Salero E and ME Hatten. (2007). Differentiation of ES cells into cerebellar neurons. Proc Natl Acad Sci USA 104:2997–3002.
11. Su HL, K Muguruma, M Matsuo-Takasaki, M Kengaku, K Watanabe and Y Sasai. (2006). Generation of cerebellar neuron precursors from embryonic stem cells. Dev Biol 290:287–296.
12. Chizhikov V and KJ Millen. (2003). Development and malformations of the cerebellum in mice. Mol Genet Metab 80:54–65.
13. Wurst W and L Bally-Cuif. (2001). Neural plate patterning: upstream and downstream of the isthmic organizer. Nat Rev Neurosci 2:99–108.
14. Alder J, NK Cho and ME Hatten. (1996). Embryonic precursor cells from the rhombic lip are specified to a cerebellar granule neuron identity. Neuron 17:389–399.
15. Sotelo C. (2004). Cellular and genetic regulation of the development of the cerebellar system. Prog Neurobiol 72:295–339.
16. Wingate RJ and ME Hatten. (1999). The role of the rhombic lip in avian cerebellum development. Development 126: 4395–4404.
17. Lin JC, L Cai and CL Cepko. (2001). The external granule layer of the developing chick cerebellum generates granule cells and cells of the isthmus and rostral hindbrain. J Neurosci 21:159–168.
18. Machold R and G Fishell. (2005). Math1 is expressed in temporally discrete pools of cerebellar rhombic-lip neural progenitors. Neuron 48:17–24.
19. Wang VY, MF Rose and HY Zoghbi. (2005). Math1 expression redefines the rhombic lip derivatives and reveals novel lineages within the brainstem and cerebellum. Neuron 48:31–43.
20. Alder J, KJ Lee, TM Jessell and ME Hatten. (1999). Generation of cerebellar granule neurons in vivo by transplantation of BMP-treated neural progenitor cells. Nat Neurosci 2:535–540.
21. McMahon AP and A Bradley. (1990). The Wnt-1 (int-1) proto-oncogene is required for development of a large region of the mouse brain. Cell 62:1073–1085.
22. Crossley PH, S Martinez and GR Martin. (1996). Midbrain development induced by FGF8 in the chick embryo. Nature 380:66–68.
23. Joyner AL, A Liu and S Millet. (2000). Otx2, Gbx2 and Fgf8 interact to position and maintain a mid-hindbrain organizer. Curr Opin Cell Biol 12:736–741.
24. Joyner AL. (1996). Engrailed, Wnt and Pax genes regulate midbrain—hindbrain development. Trends Genet 12:15–20.
25. Akazawa C, M Ishibashi, C Shimizu, S Nakanishi and R Kageyama. (1995). A mammalian helix-loop-helix factor structurally related to the product of Drosophila proneural gene atonal is a positive transcriptional regulator expressed in the developing nervous system. J Biol Chem 270:8730–8738.
26. Ben-Arie N, AE McCall, S Berkman, G Eichele, HJ Bellen and HY Zoghbi. (1996). Evolutionary conservation of sequence and expression of the bHLH protein Atonal suggests a conserved role in neurogenesis. Hum Mol Genet 5:1207–1216.
27. Yang XW, R Zhong and N Heintz. (1996). Granule cell specification in the developing mouse brain as defined by expression of the zinc finger transcription factor RU49. Development 122:555–566.
28. Liem KF Jr., G Tremml, H Roelink and TM Jessell. (1995). Dorsal differentiation of neural plate cells induced by BMP-mediated signals from epidermal ectoderm. Cell 82:969–979.
29. Dahmane N and A Ruiz i Altaba. (1999). Sonic hedgehog regulates the growth and patterning of the cerebellum. Development 126:3089–3100.
30. Gazit R, V Krizhanovsky and N Ben-Arie. (2004). Math1 controls cerebellar granule cell differentiation by regulating multiple components of the Notch signaling pathway. Development 131:903–913.
31. Borghesani PR, JM Peyrin, R Klein, J Rubin, AR Carter, PM Schwartz, A Luster, G Corfas and RA Segal. (2002). BDNF stimulates migration of cerebellar granule cells. Development 129:1435–1442.
32. Kyriakopoulou K, I de Diego, M Wassef and D Karagogeos. (2002). A combination of chain and neurophilic migration involving the adhesion molecule TAG-1 in the caudal medulla. Development 129:287–296.
33. Corrales JD, GL Rocco, S Blaess, Q Guo and AL Joyner. (2004). Spatial pattern of sonic hedgehog signaling through Gli genes during cerebellum development. Development 131:5581–5590.
34. Han J, D Kang and D Kim. (2003). Properties and modulation of the G protein-coupled K+ channel in rat cerebellar granule neurons: ATP versus phosphatidylinositol 4,5-bisphosphate. J Physiol 550:693–706.
35. Slesinger PA, N Patil, YJ Liao, YN Jan, LY Jan and DR Cox. (1996). Functional effects of the mouse weaver mutation on G protein-gated inwardly rectifying K+ channels. Neuron 16:321–331.
36. Nakatsuji N and I Nagata. (1989). Paradoxical perpendicular contact guidance displayed by mouse cerebellar granule cell neurons in vitro. Development 106:441–447.
37. Solecki DJ, EE Govek, T Tomoda and ME Hatten. (2006). Neuronal polarity in CNS development. Genes Dev 20:2639–2647.
38. Appel B and JS Eisen. (2003). Retinoids run rampant: multiple roles during spinal cord and motor neuron development. Neuron 40:461–464.
39. Sockanathan S, T Perlmann and TM Jessell. (2003). Retinoid receptor signaling in postmitotic motor neurons regulates rostrocaudal positional identity and axonal projection pattern. Neuron 40:97–111.
40. Komine O, M Nagaoka, K Watase, DH Gutmann, K Tanigaki, T Honjo, F Radtke, T Saito, S Chiba and K Tanaka. (2007). The monolayer formation of Bergmann glial cells is regulated by Notch/RBP-J signaling. Dev Biol 311:238–250.
41. Itsykson P, N Ilouz, T Turetsky, RS Goldstein, MF Pera, I Fishbein, M Segal and BE Reubinoff. (2005). Derivation of neural precursors from human embryonic stem cells in the presence of noggin. Mol Cell Neurosci 30:24–36.
42. Hatten ME, AM Francois, E Napolitano and S Roffler-Tarlov. (1984). Embryonic cerebellar neurons accumulate

[3H]-gamma-aminobutyric acid: visualization of developing gamma-aminobutyric acid-utilizing neurons in vitro and in vivo. J Neurosci 4:1343–1353.
43. Wassef M, JP Zanetta, A Brehier and C Sotelo. (1985). Transient biochemical compartmentalization of Purkinje cells during early cerebellar development. Dev Biol 111:129–137.
44. Dupont JL, E Fourcaudot, H Beekenkamp, B Poulain and JL Bossu. (2006). Synaptic organization of the mouse cerebellar cortex in organotypic slice cultures. Cerebellum 5:243–256.
45. Semyanov A, MC Walker, DM Kullmann and RA Silver. (2004). Tonically active GABA A receptors: modulating gain and maintaining the tone. Trends Neurosci 27:262–269.
46. De Filippi G, T Baldwinson and E Sher. (2001). Evidence for nicotinic acetylcholine receptor activation in rat cerebellar slices. Pharmacol Biochem Behav 70:447–455.
47. Martin-Ruiz CM, M Lee, RH Perry, M Baumann, JA Court and EK Perry. (2004). Molecular analysis of nicotinic receptor expression in autism. Brain Res Mol Brain Res 123:81–90.
48. Zoghbi HY and HT Orr. (1995). Spinocerebellar ataxia type 1. Semin Cell Biol 6:29–35.

Address correspondence to:
Dr. Slaven Erceg
CABIMER (Centro Andaluz de Biología Molecular y Medicina Regenerativa)
Avda. Americo Vespucio s/n
Parque Científico y Tecnológico Cartuja
Sevilla
Spain

E-mail: serceg@cipf.es

Dr. Miodrag Stojkovic
Department of Human Genetics
Medical School, University of Kragujevac
Kragujevac
Serbia

E-mail: mstojkovic@spebo.co.rs

Received for publication December 11, 2009
Accepted after revision June 2, 2010
Prepublished on Liebert Instant Online June 3, 2010